Journal of Manufacturing Processes 11 (2009) 38–44

Contents lists available at ScienceDirect

Journal of Manufacturing Processes

journal homepage: www.elsevier.com/locate/manpro

Technical paper

Application of vibration in the laser powder deposition process

Ehsan Foroozmehr, Dechao Lin, Radovan Kovacevic *

Center for Laser Aided Manufacturing (CLAM), Southern Methodist University, Dallas, TX 75205, USA

ARTICLE INFO

Article history:
Received 26 October 2008
Received in revised form
28 January 2009
Accepted 12 July 2009
Available online 23 July 2009

ABSTRACT

Laser powder deposition (LPD) has been used for a few decades as a technique that is unique in the application of complex geometry part manufacturing, high-value parts repairing, and surface modification. However, improving the buildup quality of LPD process is still a challenge because of the presence of defects. In this paper, the effect of in-process vibration frequency on the buildup properties of LPD is studied. Experimental results show that the vibratory energy has a significant effect on reducing porosity. Up to an 80% reduction in the porosity and the maximum defect size can be obtained by choosing the appropriate vibration parameters. In addition, a more homogeneous microstructure is achieved that results in less deviation in hardness throughout the buildup.

1. Introduction

For many years, near-net-shape fabrication using laser technology has opened an extensive research area. Different aspects of this process, such as the feasibility to make near-net-shape parts [1,2], process planning and controlling [3,4], thermo-mechanical modeling, [5,6] and thermo-kinetic modeling [7] of the process have been investigated by a number of researchers. The quality of the process with the aid of real time monitoring and process control can be improved. However, the dynamic nature of the process and level of sensitivity to the process parameters require other techniques to enhance the quality of the buildups. Porosity is one of the recurrent problems in the LPD process. Based on their shape and location, two types of porosity have been reported [8]. Close to the intersection of the beads, the first type of porosity occurs because of a lack of fusion or unmelted particles. Gas porosity is the other type that happens because of trapped gas which is dispersed randomly throughout the buildup.

In-process vibration as an auxiliary technique has been used to improve the quality of the casting and welding processes. The application of vibration in the casting of metals has a history dating back to the 1950s [9] and 1960s [10] when it was claimed that vibration could change the microstructure of parts, improve mechanical properties, and reduce defects. Similar observations were obtained in more recent investigations on the casting of aluminum alloys and steels [11–14]. Vibratory energy tends to homogenize the dendritic structure by breaking the dendrite arms during solidification. This breakage creates a finer microstructure in the part. In addition, the amount of cavity and porosity shrinkage is decreased [13] by applying vibration. Fatigue and impact properties of the parts are also reported to be enhanced in vibration-assisted castings [11]. Surface roughness of the casted parts is reported to be less when vibration is applied during casting [14]. In welding, vibration has been used to refine the grain structure of the weld as well as to improve the mechanical properties of the weld joints by decreasing the tensile residual stress [15–18]. The shrinkage cavity problem is also reported to be diminished by applying vibration during laser cladding of ceramic-metal composite on Al-alloys [19]. In the present work, an electromagnetic driven vibrator was manufactured in the Center for Laser Aided Manufacturing (CLAM) to study the effect of in-process vibration on the porosity level, micro-hardness distribution, and microstructure of LPD buildups.

2. Experimental setup and procedures

To investigate the in-process mechanical vibration on the quality of laser cladding, a vibration system is integrated into the laser-cladding system, which consists of : (1) a 1-kW Nd:YAG laser system with a laser head capable to deliver the powder, (2) a 5-axis CNC vertical machining center with a laser head attached to the *Z*-axis, (3) a powder feeding system capable of delivering metal powder with the protective argon gas flow, and (4) the vibrator setup, which is placed on the *x*–*y*-table of the CNC vertical machining center. The schematic of the vibrator system is shown in Fig. 1. An electromagnetic shaker [20] is tightly connected to an aluminum plate (shown in Fig. 2) that is placed on the *x*–*y* table of the CNC machine. The frequency of the vibration is controlled by a signal generator that is connected to a 400-W amplifier. The shaker is equipped with an accelerometer that is connected to a data acquisition system to monitor the vibrator parameters.

* Corresponding author. Tel.: +1 214 768 4865; fax: +1 214 768 0812.
E-mail addresses: eforoozmeh@smu.edu (E. Foroozmehr), dlin@mail.smu.edu (D. Lin), kovacevi@engr.smu.edu (R. Kovacevic).

1526-6125/$ – see front matter © 2009 The Society of Manufacturing Engineers. Published by Elsevier Ltd. All rights reserved.
doi:10.1016/j.jmapro.2009.07.002

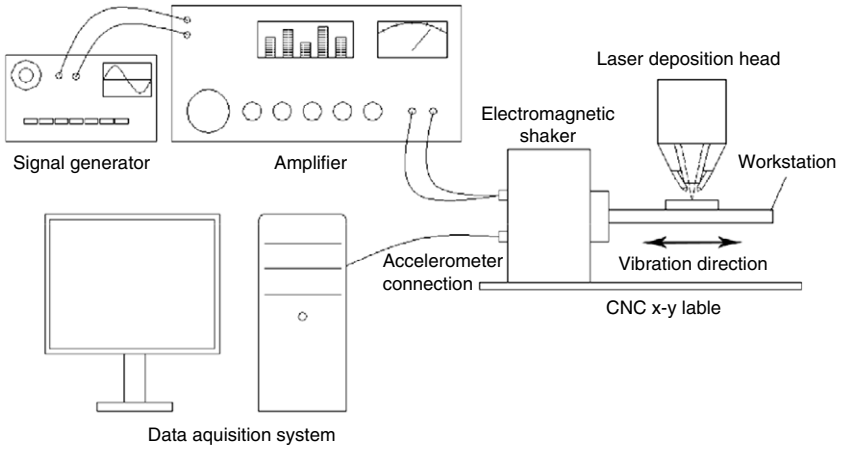

Fig. 1. Schematic representation of the in-process vibration-assisted laser powder deposition.

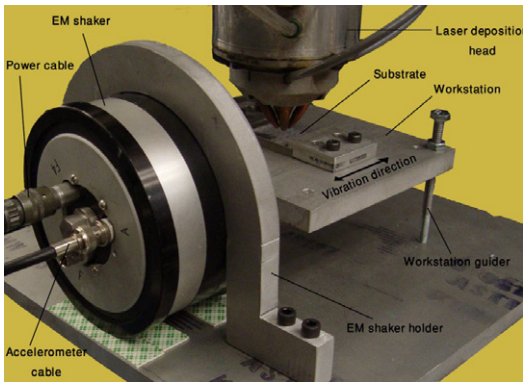

Fig. 2. Assembly of the electromagnetic vibrator.

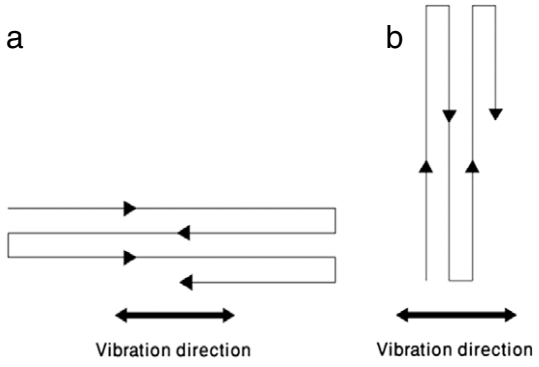

Fig. 3. Definition of vibration direction vs. cladding path, (a) Parallel vibration, (b) Lateral vibration.

2.1. Sample preparation and evaluation

A CNC program is developed to define the deposition path and the process parameters. Based on the previous experiences in deposition of AISI H13 powder with MultiFab[1] system, the process parameters are chosen in a way that an optimum deposition in terms of clad geometry and deposition rate is obtained. Therefore, the laser power, laser scanning speed, and powder feeding rate are kept constant and equal to 390 W, 9 mm/s, and 4.6 g/min, respectively. By measuring the powder mass flow rate and the net deposition rate, the powder efficiency during the experiments is estimated to be 20%. Three vibration frequencies of 75, 150, and 300 Hz with amplitudes of 197-, 56-, and 21-μm, respectively, and two vibration directions of parallel and lateral are chosen. The vibration direction is defined with respect to the deposition direction. In parallel vibration, the vibration direction is parallel to the deposition path (Fig. 3(a)); and in lateral vibration, the vibration direction is perpendicular to the deposition path (Fig. 3(b)). In each experiment, a coupon with dimensions of 15 × 5.5 × 4.5 mm (10 layers and 15 beads in each layer) from AISI H13 powder with a mesh size of −80/+325 is made on a substrate of AISI 4140.

After performing the experiments, each coupon is cut along the traverse direction (perpendicular to the deposition direction), mounted, ground, and polished. Mirror surface is completed by using 5- to 1-micron alumina suspensions in distilled water. An etchant of 2% nital is used to reveal the prior-austenite grain boundaries, which are suitable for alloy steels like H13 [21]. An optical metallurgical and scanning electron microscope (SEM) is used to study the effect of vibration on grains growth.

Studying the porosity is based on quantifying the amount of porosity in the randomly sectioned samples. For this purpose, an optical digital microscope is used with 50x magnification. The brightness of the microscope is adjusted so that a proper contrast between the pores and the surrounding material can be detected. Fig. 4(a) shows a captured picture of the cross-section of a polished coupon. The captured images are processed to remove the extra glare around the section and increase the sharpness of the colors, as shown in Fig. 4(b). The histogram of this image (Fig. 5) is used to define the number of pixels of each color in gray-scale mode. In gray-scale mode, the color numbers range from 0 for black to 255 for white. The summation of pixels for color numbers 0 to 40 divided by the total number of pixels is calculated to define the porosity percentage for all experiments. For example, for the experiment performed under non-vibratory situation, the number of pixels for color numbers from 0 to 40 is 21 887 and the total number of pixels is 1728 818, resulting in 0.96% porosity (shown in Fig. 7). The maximum pore size is also studied by comparing the diameter of an equivalent circle with an area equal to the detected maximum defect area in the image of the cross-section. Because this method is based on the areas under study, the results can be either under-estimated or over-estimated. Nonetheless, the results can provide a qualitative comparison for different experiments.

[1] Multi Fabrication system, is a hybrid multi-functional system for rapid manufacturing and repair that has been developed in Research Center for Advanced Manufacturing (RCAM) in SMU.

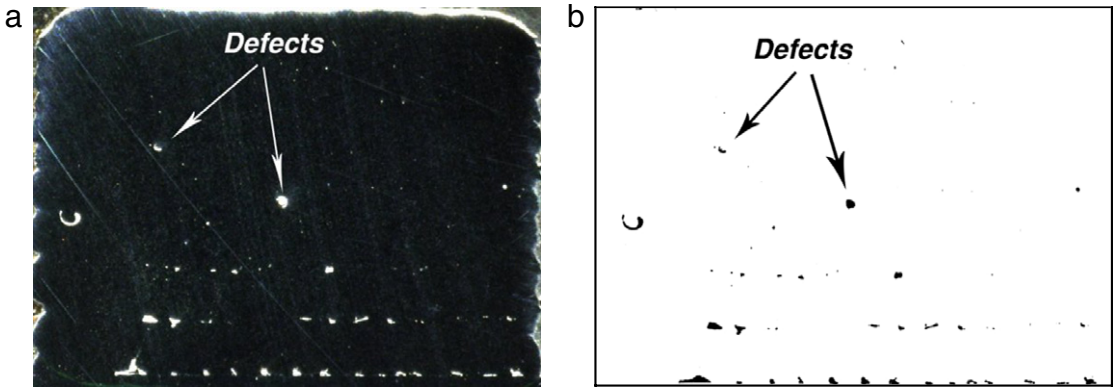

Fig. 4. Processing of optical microscope image. (a) Original image captured by optical microscope. (b) Processed image.

Fig. 5. Histogram of the processed image in Fig. 4(b).

Micro-hardness test is performed from the buildup–substrate interface up to the top of the part to study the effect of vibration on hardness distribution throughout the buildup. The indentation distance is 150 μm under a 200-g load.

3. Results and discussion

3.1. Effects of vibration on the mitigation of defects

Two different types of defects can be classified in the components made by the LPD process. One type, usually located along the intersection of the beads, has an irregular shape with various geometry and sizes. This type of defect can be caused by unmelted particles (Fig. 6(a)) or by lack of fusion (Fig. 6(b)). The other type of defect is the spherical-like trapped gas porosity that is distributed randomly (Fig. 6(c)).

Referring back to Fig. 5, it can be concluded that the amount and size of the defects decrease at higher layers from the substrate. This phenomenon can be contributed to the higher cooling rate at the beginning of the process. At the higher layers, the molten pool becomes larger and is characterized by a slower solidification rate. Therefore, the defects due to lack of fusion and unmelted particles are less likely to happen.

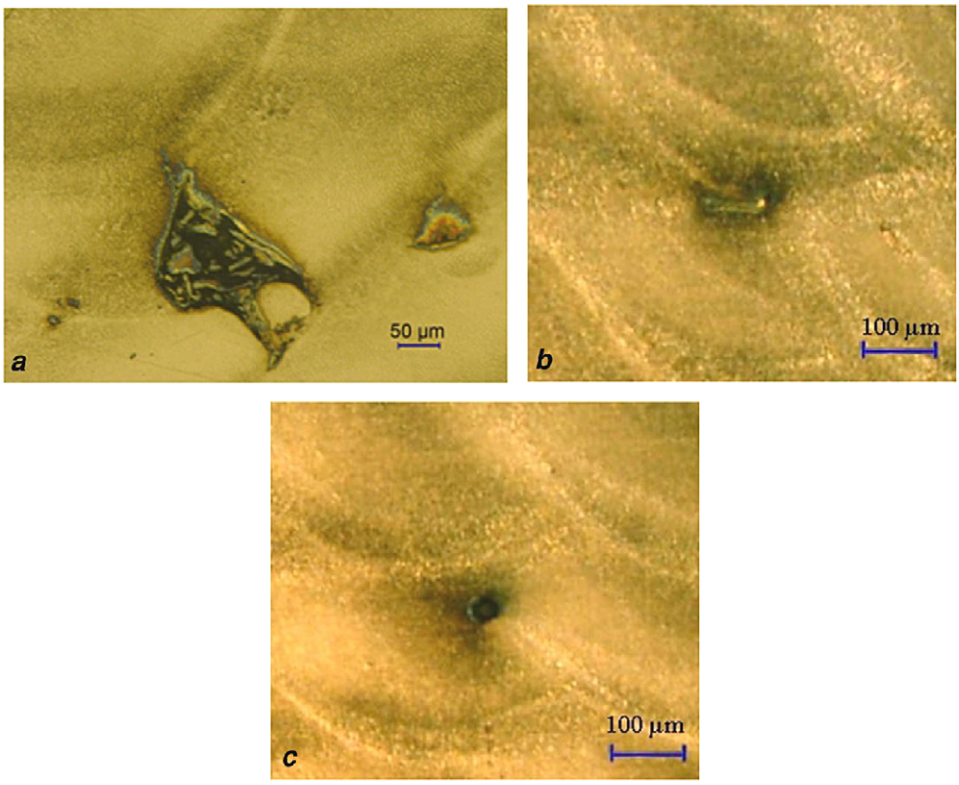

Fig. 6. Classification of defects in the LPD process, (a) unemlted particle, (b) lack of fusion, (c) trapped gas.

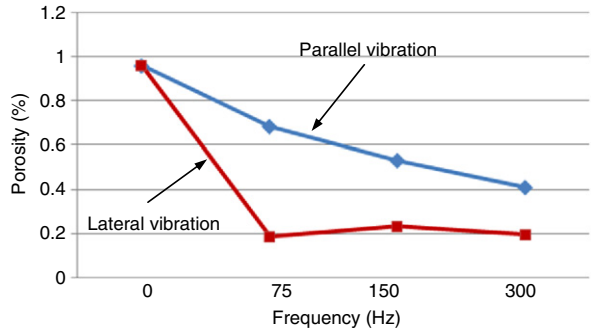

Fig. 7. Effect of vibration frequency and direction on porosity.

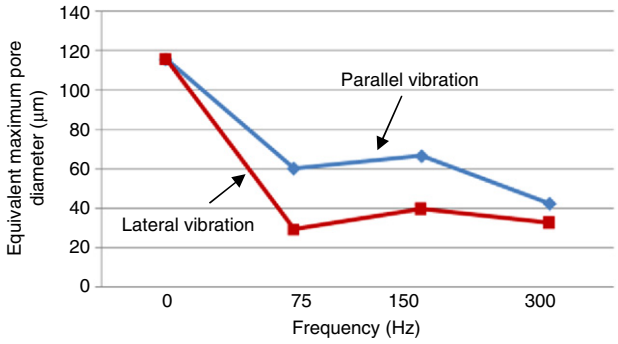

Fig. 8. Effect of vibration frequency and direction on equivalent maximum pore diameter.

The performed experiments under vibratory conditions show a significant effect on reducing the porosity level of buildups. Fig. 7 compares the effect of vibration frequency on the intensity of porosity for both the parallel and lateral vibration directions. As can be seen, the porosity percentage is decreased to about 60% ($[0.96 - 0.40] * 100/0.96 = 58.3\%$) in the parallel vibration and about 80% ($[0.96 - 0.2] * 100/0.96 = 79.1\%$) in the lateral vibration. The effect of lateral vibration on reducing the porosity is relatively independent of the applied frequency. However, the parallel vibration shows a continuously decreasing trend by increasing the frequency.

A similar trend is observed in the equivalent maximum pore diameter results. As can be seen in Fig. 8, the maximum defect size in parallel vibration is decreased about 50% ($[115.9 - 60.5] * 100/115.9 = 47.8\%$) in 75 and 150 Hz and about 65% ($[115.9 - 42.6] * 100/115.9 = 65.6\%$) in 300 Hz. In lateral vibration, the maximum defect size is decreased about 75% ($[115.9 - 29.6] * 100/115.9 = 74.5\%$) in 75 Hz and about 65% ($[115.9 - 39.2] * 100/115.9 = 66.1\%$) in 150 and 300 Hz. The non-uniformity in the trend of results can be contributed to the random nature of the measured data. Nonetheless, the relatively stable results of the maximum defect size under vibratory conditions prove the capability of the vibratory energy to mitigate the size of the defects and their number in the LPD process.

3.2. Effect of vibration on the microstructure of the buildup

Fig. 9(a) shows the cross-section of the buildup after etching in 2% nital. One of the beads is enlarged in this figure, and three zones are distinguished with letters A, B, and C. Zones A and C are close to the fusion line while zone B is in the middle of the bead. A higher magnification of zones A and C are shown in Fig. 9(b) and (c), respectively. From these figures, it can be seen that the columnar grains grow perpendicularly from the fusion line along the maximum temperature gradient line toward the central region. Fig. 9(d) shows that the grain structure in the middle of the bead is characterized with the presence of equiaxed grains, indicating the central region has larger undercooling during the solidification process. This structure in a cladding bead is similar to the one in fusion welding.

When the experiments are performed under vibration, a substantial change in the dendritic zones is observed. The dendritic structure (along the fusion line from zone A to C) for parallel and lateral vibration under different frequencies is shown in Figs. 10 and 11, respectively. As can be seen in Fig. 10, under a vibratory situation, the length of the dendrite arms has decreased, the width of dendrite arms has slightly increased, and the number of dendrite secondary arms has increased for all applied frequencies of parallel vibration. These effects become more noticeable under higher frequencies. A similar trend is observed by looking at the lateral vibration in Fig. 11. The vibration energy seems to have the potential to break the dendrite arms by disturbing the fluid flow during solidification. In addition, the slightly increased width of the grains as well as the increased number of secondary dendrites can result from the decrease of the temperature gradient from the fusion line to the center of the bead [22], caused by disturbances of the vibration. The broken dendrite pieces are transported with the fluid flow and work as new nuclei. The broken dendrites will grow along their original direction, which may cause some randomly oriented grains (Fig. 12). It is shown by the authors [23] that as a result of the broken dendrites being transported with the fluid flow and the reduction in the temperature gradient, the average size of the equiaxed grains (in zone C) increases under vibratory LPD.

Finer grain materials with more grain boundary regions have typically higher strength and ductility [24]. Therefore, the effect of vibration on reducing the grain size and increasing the grain boundary regions can enhance the mechanical properties of the buildup. Further research is needed to prove this effect in the LPD process.

3.3. Effect of vibration on the hardness distribution

The measurement of micro-hardness is performed at the cross-section of the buildup along a vertical line from the buildup–substrate interface to the top of the buildup by using a micro-hardness tester. Fig. 13 shows the micro-hardness distribution for the experiments made under parallel vibration and without vibration. The solid line in Fig. 13 represents the case without vibration. Two regions can be distinguished (separated by dashed line): one region starts from the bottom of the buildup to a height of 3 mm. This region is characterized by the lower average hardness. The other region from the 3 mm height to the top of the buildup and is characterized with a higher average hardness than the first region. Multiple heating–cooling cycles due to multiple beads in each layer as well as the deposition of subsequent layers result in tempering the bottom layers; and consequently, less hardness is expected for this region. However, the last few beads on the top region are exposed to less thermal cycles; therefore, a higher average hardness is obtained, which is similar to the report in the literature [25]. A similar trend can be seen in Fig. 14 for the experiments performed under lateral vibration.

Although the range of distribution of the hardness values in the first region (from the bottom of the buildup to a 3 mm height) is between 490 to 570 HV for all applied vibration frequencies and directions, by careful attention to the hardness values, it is revealed that less variation in the hardness values is obtained for the buildups made with vibration than for the buildups made without vibration. In order to clarify this effect, the standard deviation (Eq. (1)) of the hardness data from the bottom to the 3 mm height (first region) for both parallel and lateral vibrations is shown in Fig. 15.

$$S_N = \sqrt{\frac{1}{N}\sum_{i=1}^{N}(x_i - \bar{x})^2} \quad (1)$$

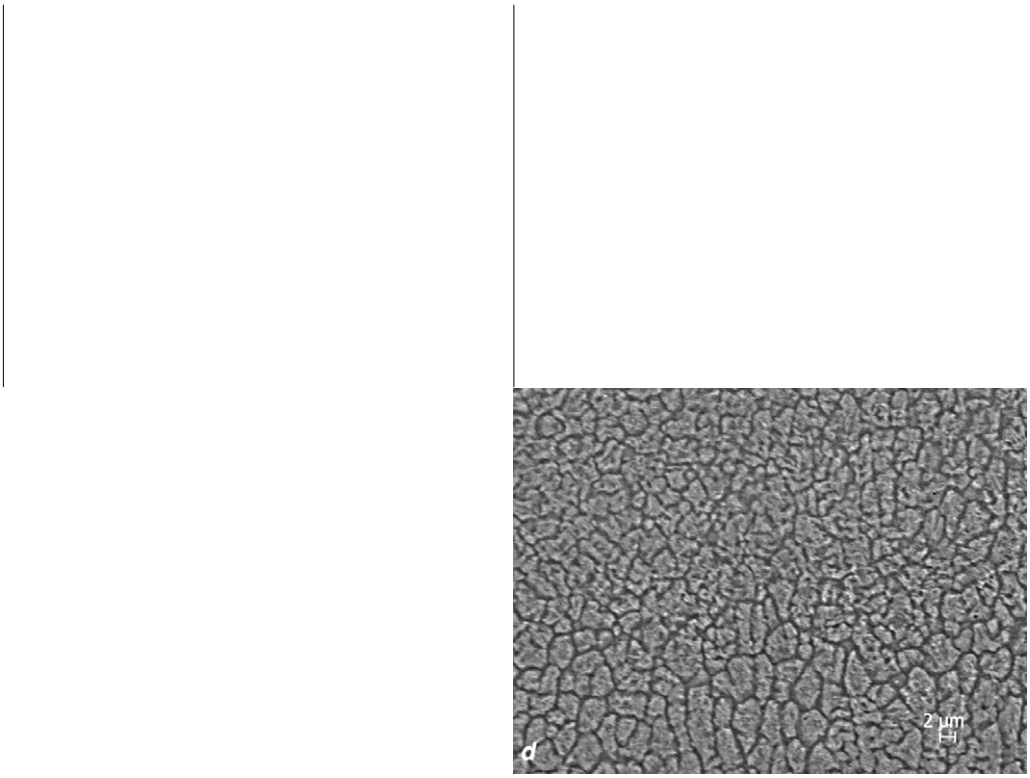

Fig. 9. The typical microstructures of a single bead in various regions. (a) Overall cross-section of the buildup and an enlarged bead. (b) Higher magnification of zone A. (c) Higher magnification of zone C. (d) Higher magnification of zone B.

Fig. 10. Micrographs of the columnar dendrite at zone A under parallel vibration. (a) Vibration frequency: 75 Hz. (b) Vibration frequency: 150 Hz. (c) Vibration frequency: 300 Hz.

where, N is the number of data, x_i is the hardness value at each point, and $\bar{x}$ is the average hardness. As can be seen in Fig. 15, the standard deviation of hardness has noticeably reduced in all applied frequencies and directions. However, as the amplitude is reduced in higher frequencies, it shows less effect by increasing the frequency to 300 Hz. This effect can be explained by referring back